Overexpression of CD40 Ligand in Murine Epidermis Results in Chronic Skin Inflammation and Systemic Autoimmunity

Annette Mehling, Karin Loser, Georg Varga, Dieter Metze, Thomas A. Luger, Thomas Schwarz, Stephan Grabbe, and Stefan Beissert

Ludwig Boltzmann Institute for Cell Biology, Department of Dermatology and Immunology of the Skin, University of Münster, D-49149 Münster, Germany

Abstract

CD40–CD40 ligand (L) interactions play a pivotal role in immune-mediated inflammatory responses via the activation of antigen-presenting cells (APCs). To investigate the effects of continuous activation of resident tissue APCs, in this case the Langerhans cells (LCs) of the skin, CD40L expression was targeted to the basal keratinocytes of the epidermis of mice using the keratin-14 promoter. Approximately 80% of the transgenic (Tg) mice spontaneously developed dermatitis on the ears, face, tail, and/or paws. Compared with littermates, Tgs had a >90% decrease in epidermal LCs yet increased numbers within the dermis suggestive of enhanced emigration of CD40-activated LCs. Tgs also displayed massive regional lymphadenopathy with increased numbers of dendritic cells and B cells. Moreover, a decrease in IgM and an increase in IgG1/IgG2a/IgG2b/IgE serum concentrations was detectable. Screening for autoantibodies revealed the presence of antinuclear antibodies and anti-dsDNA antibodies implicative of systemic autoimmunity. Accordingly, renal Ig deposits, proteinuria, and lung fibrosis were observed. Adoptive transfer of T cells from Tgs to nonTg recipients evoked the development of skin lesions similar to those found in the Tgs. Dermatitis also developed in B cell–deficient CD40L Tg mice. These findings suggest that in situ activation of LCs by CD40L in the skin not only leads to chronic inflammatory dermatitis but also to systemic mixed-connective-tissue-like autoimmune disorders, possibly by breaking immune tolerance against the skin.

Key words: Langerhans cell • autoantibody • transgenic mice • mixed connective tissue disease • migration

Introduction

One of the initial steps in the induction of immune reactions is the transport of antigen to the lymph node by APCs, in particular dendritic cells (DCs)*. Immature DCs, such as the Langerhans cells (LCs) of the epidermis, predominantly reside in peripheral tissues where they build a network of sentinel cells that can acquire and process foreign antigens. Upon encountering exogenous antigens, they mature and migrate to secondary lymphoid organs where they present antigens to T cells. Only DCs have the unique capacity to present antigens in the proper context of the antigenic and costimulatory molecules required to prime naive T cells (1). These costimulatory molecules include the members of the TNF/TNF-R family, the B7 family, and others. However, engagement of TNF/TNF-R family molecules also induces activation and maturation of DCs. In this respect, triggering of CD40 on DCs by CD40L-expressing activated $CD4^+$ T cells is one of the strongest DC-activating signals known, and it has been suggested that CD40–CD40L interactions are critical for T cell help (2). In addition to DCs, CD40 is also prominently expressed on B cells, where it plays an important role in germinal center formation, isotype switching, and B cell survival (3, 4).

In this study, the in vivo effects of continuous in situ activation of tissue-specific resident APCs, the exemplary model being the activation of epidermal DCs via CD40–CD40L interactions, were examined in a transgenic (Tg) mouse model. For this purpose, CD40L expression was targeted to the basal keratinocytes using a keratin-14 expression cassette. Tg mice developed spontaneous inflammatory skin lesions, which showed histopathologic features of

Address correspondence to Stefan Beissert, Dept. of Dermatology, University of Münster, Von Esmarch Strasse 58, D-48149 Münster, Germany. Phone: 49-251-835-6582; Fax: 49-251-835-8579; E-mail: beisser@uni-muenster.de

**Abbreviations used in this paper:* ANA, antinuclear antibody; DC, dendritic cell; H&E, hematoxylin and eosin; HRP, horseradish peroxidase; L, ligand; LC, Langerhans cell; Tg, transgenic.

J. Exp. Med. © The Rockefeller University Press • 0022-1007/2001/09/615/14 $5.00
Volume 194, Number 5, September 3, 2001 615–628
http://www.jem.org/cgi/content/full/194/5/615

chronic autoimmune disease. Ear sheets stained for I-A$^+$ LCs revealed an almost complete depletion (>90%) of LCs in the epidermis and a profound in situ activation of the remaining LCs in Tg mice compared with littermates. Increased numbers of activated DCs were present in the dermis and in skin-draining lymph nodes, suggesting that activated LCs emigrate at a higher rate from skin to draining lymph nodes. Tg mice also displayed massive regional lymph node hyperplasia and splenomegaly with increased numbers of DCs and B cells. Remarkably, CD40L Tgs developed a systemic autoimmune disease as evidenced by the presence of autoantibodies including anti-dsDNA-antibodies and autoreactive T cells. These disorders were accompanied by internal organ involvement, such as renal Ig deposits, proteinuria, and inflammatory lung fibrosis. Accordingly, these animals had a significantly shorter life expectancy and finally succumbed to their disease. Transfer of CD8$^+$ T cells from Tg mice to naive wild-type mice resulted in the development of autoimmune skin inflammation in the recipients. These findings indicate that in situ expression of CD40L in the skin not only leads to chronic inflammatory (autoimmune) dermatitis, but surprisingly also to systemic mixed-connective-tissue-like autoimmune disorders. Thus, these data point to a possible role of activated DCs in the development of autoimmunity possibly by breaking immune tolerance against tissues.

Materials and Methods

Transgene Construction and Production of Tg Mice. The gene for murine CD40 ligand (CD40L; provided by Immunex Corp.) was placed under the control of the human K14 promoter (5, 6) using standard methods as follows. The K14 expression cassette used included the K14 promoter, a rabbit β-globin intron, a multiple cloning site, and the K14 polyadenylation site (7). The SalI/XbaI fragment of the cDNA of CD40L was cloned into the SalI/XbaI restriction site of the modified expression cassette thus creating pAMM16. Plasmid DNA to be used for microinjections was purified twice using the JetStar Maxiprep Kit (Genomed). The expression cassette was digested with EcoRI/HindIII, extracted from the agarose gel using the Jetsorb Kit (Genomed), resuspended in 10.0 mM Tris-HCl/0.1 mM EDTA, pH 7.4, and used for microinjection into C57BL/6 × DBA F2 oocytes. Tg mice were identified by either PCR (AM9: GTTCAGAGTTTGAGTAAGCCA; AM28: CAATGATATACACTGTTTGAGATGA; cycling profile: 95°C for 5 min; [95°C for 1 min; 55°C for 40 s; 72°C for 1 min × 30; 72°C for 2 min]) or Southern blot analysis of DNA isolated from tail. Three founder lines were established by breeding into a DBA background. The line with the highest Tg expression was selected for more extensive analysis. Most experiments were carried out using heterozygous mice. Mice were housed under specific pathogen free conditions according to institutional regulations.

Histology and Immunohistochemical Staining. Tissues were fixed in formalin and embedded in paraffin. Hematoxylin and eosin (H&E) staining was performed by standard methods. Immunohistochemistry was performed on cryostat sections (3–8 μm) fixed in acetone according to standard methods. Slides were incubated in the appropriate dilution of monoclonal antibody or isotype control and subsequently incubated with a horseradish peroxidase (HRP)-coupled secondary antibody (Dianova). Peroxidase activity was visualized using 3-amino-9-ethyl-carbazol as a chromogen. Tissues were counterstained with MAYER'S hemalum solution (Merck KgaA). For further evaluation of the density of LCs by electron microscopy, skin biopsies were fixed in Karnovsky's solution, postfixed in 1% osmium tetroxide, embedded in epon, ultrathin cut, and counterstained with uranyl acetate and lead citrate.

Cell Preparations and Flow Cytometry. Before flow cytometric analyses, spleens and LNs were rubbed through a cell strainer. To lyse erythrocytes, spleen cell suspensions were gently agitated in lysis-buffer. Expression of cell surface molecules was quantitated by flow cytometry according to standard methods as follows. Cells were incubated with monoclonal antibody against murine pan macrophages (clone BM8; BMA Biomedicals AG): CD4 (RPA-T4; BD PharMingen); CD8 (RPA-T8; BD PharMingen); CD11c (N418; Endogen); CD19 (ID3; BD PharMingen), CD40 (HM40-3; BD PharMingen), CD40L (MR1; BD PharMingen); CD62L (Dreg 56; BD PharMingen), or I-A (clone M5/114; Roche Diagnostics) and labeled with FITC-conjugated goat anti–rat IgG or goat anti–hamster IgG (BD PharMingen or Dianova, respectively). Propidium iodide (100 nM; Sigma-Aldrich/PBS) was added to detect dead cells. The cells were subsequently analyzed in an EPICS-XL™ flow cytometer (Beckman Coulter).

Immunofluorescent Staining of Epidermal Ear Sheets. Epidermal sheets were stained essentially as described previously (8). In brief, ears were mechanically split into dorsal and ventral sides, incubated in 20 mM EDTA, pH 7.3, washed with PBS, and fixed in acetone. Sheets were incubated in 1% BSA/PBS and stained with the antibody overnight. Sheets were then incubated with a FITC-coupled secondary antibody, mounted onto slides, and examined using a Zeiss Axiovert microscope. Stained cells were quantitated by microscopy. Positive cells in at least 16 randomly selected visual fields of ocular grid of known area per ear were counted.

Assay for Antinuclear Antibodies and Autoantibodies against dsDNA. Serum samples were screened for the presence of antinuclear antibodies (ANAs) by indirect immunofluorescence on HEp-2 cells (LD Labor Diagnostika). In brief, sera were diluted in PBS before use, applied to the slides, and incubated overnight. Slides were then incubated with FITC-coupled mouse Igs (Dianova), washed, and mounted. Staining patterns were assessed at 1:80 or 1:100 dilutions. Sera were screened for the presence of anti-dsDNA antibodies using commercially available *Crithidia lucilidae* slides (The Binding Site Ltd.). Sera were applied to the slides at dilutions of 1:40. The slides were then incubated for 30 min with FITC-coupled mouse Igs (Dianova), washed, mounted, and examined using a Zeiss Axiovert microscope.

Quantification of Serum Igs and Cytokines. Levels of serum Igs were quantitated using the ELISA-based Clonotyping System HRP (Southern Biotechnology Associates, Inc.). Serum Igs were detected with HRP-coupled antibodies specific for mouse IgA, IgG1, IgG2a, IgG2b, IgG3, IgM, and IgE. To determine differences in cytokine expression, serum or cell supernatants were assayed by ELISA using the following antibody sets: IFN-γ; IL-4; IL-6; IL-12; and TNF-α (OPTEIA assays; all from BD PharMingen).

Detection of Ig Deposits. Renal Ig deposits were detected on cryostat sections of kidneys stained with FITC-coupled mouse Igs (Dianova) diluted 1:30 in 0.9% saline solution. Ig deposits in the skin were detected by a modified method described previously (9, 10). Cryostat sections were incubated with 1:10 dilutions of serum and 1:100 dilutions of FITC-conjugated anti–

mouse Igs (Dianova). Sections were mounted and examined using a Zeiss Axiovert microscope.

Adoptive T Cell Transfer and Serum Transfer. T cells ($CD4^+$, $CD8^+$, and $CD4^+$ $CD8^+$) were prepared from spleens and LNs of CD40L Tg or age- and sex-matched control mice. LNs and spleens were rubbed through a cell strainer and the resulting cell suspension was prepurified by passing it over a nylon wool column. Subsequently, T cells were enriched by negative selection using antibodies against non-T cells and separation via the MACS® technology as follows. Cells were incubated with the antibodies anti-CD11b (M1/70), anti-CD16/32 (2.4G2), anti-CD24 (M1/69), anti-CD45/B220 (RA3-6B2), anti–Gr-1/Ly-6G (RB6-8C5), anti–γδ-T cells (GL3), anti–NK T cells (U5A2-13), anti-CD4 (H129.19), or anti-CD8 (53-6.7), respectively (all purchased from BD PharMingen) for 15 min at 4°C and subsequently washed twice with PBS/1% FCS. Antibody-labeled cells were then incubated for another 15 min at 4°C with anti–rat antibodies conjugated with magnetic beads (Milteny Biotec). After washing the cells twice with PBS/1% FCS/2 mM EDTA antibody-labeled cells were separated via magnetic cell sorting (MACS®; Miltenyi Biotec). The negative fraction was stained with antibodies for T cells and analyzed by flow cytometry. Purity of T cells ($CD3^+$) was 94.4%, 89.2% for $CD4^+$, and 87.6% for $CD8^+$ T cells. 10^7 $CD4^+$, or $CD8^+$ T cells were injected intravenously into 5–6-wk-old sex-matched (C57BL/6 × DBA/F1) recipient control mice ($n = 6$). Mice were monitored for 6 wk.

Serum was prepared from Tg or nonTg mice and 150 μl were injected intravenously into nonTg mice ($n = 6$). Mice were monitored for 6 wk.

Tracking of LC Migration. Migration of LCs was monitored using FITC as a tracer as described previously (11–13). In brief, ears were treated with FITC (500 μg/15 μl dibutylphtalate/acetone 1:1 supplemented with 5% DMSO; Sigma-Aldrich). The retroauricular and cervical LNs were prepared 18 h later. Single cell suspensions were stained for CD11c and subjected to flow cytometric analyses.

Statistical Evaluation. The significance of differences between the mean values obtained for cytokine and Ig experiments was assessed by the two-tailed Student's *t* test for unpaired data. Lifespan data was plotted using Kaplan and Meier curves and significances were evaluated using a log-rank test. *P* values <0.05 were regarded as being significant.

Results

Generation and Phenotype of CD40L Tg Mice. To activate LCs in vivo, CD40L expression was targeted to the epidermis of mice using the keratin-14 expression cassette shown in Fig. 1 A. The expression of genes using this cassette has been widely studied (14–17). The K14 promoter drives the expression of genes in most basal cells of stratified squamous epithelium including the epidermis, oral epithelium, and palmoplantar skin (16, 18). Most of the noncoding sequences of the CD40L cDNA were removed before insertion into the expression cassette as these could play a role in posttranscriptional regulation of the gene (19). Founders were identified by PCR and Southern blot analyses. To ascertain whether the transgene was being correctly expressed, immunohistochemical analyses of cryostat sections of ears using an anti-CD40L antibody were performed. A strong and uniform expression of CD40L by the basal keratinocytes was detected in epidermis of CD40L Tg mice (Fig. 1 B). No expression was detectable in the dermis or epidermis of nonTg mice. Tg expression followed the

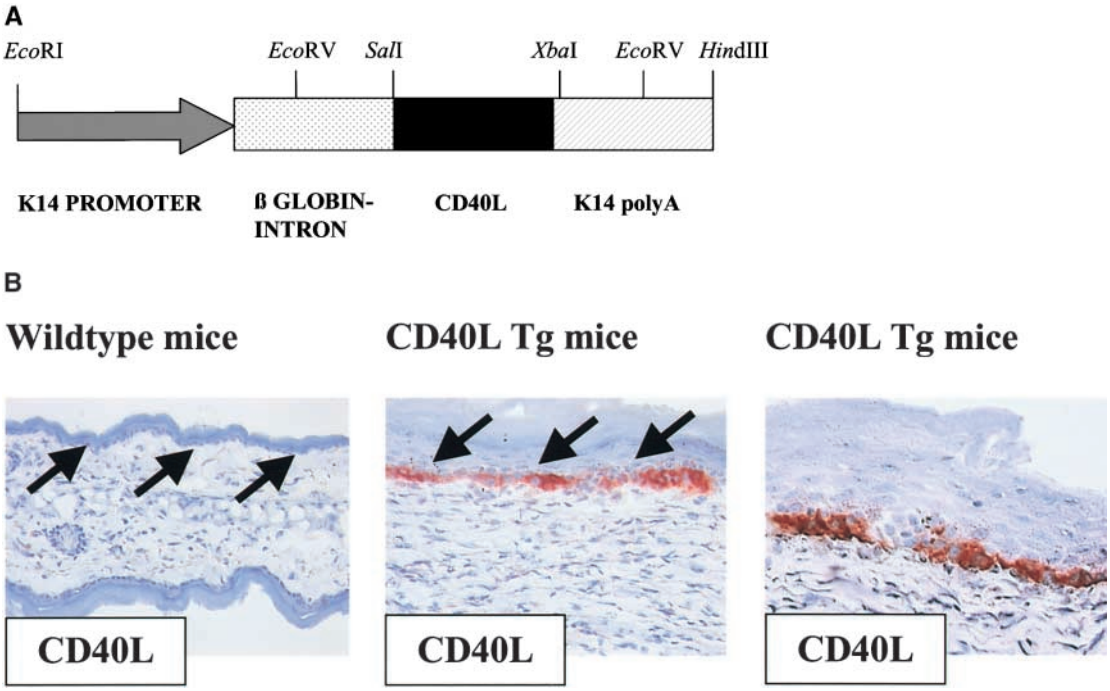

Figure 1. (A) K14/CD40L expression cassette used for the generation of the Tg mice. The construct contains the K14 promoter (arrow), the β-globin intron (dotted box), the CD40L-cDNA (black box), and the K14 poly A^+ (hatched box). (B) Immunohistochemical staining of ear skin using an antibody directed against CD40L. Arrows point to the basal keratinocytes of the epidermis. Original magnification (left to right): 40×; 200×; 400×.

expected pattern in other tissues as has been described in detail before (16) and, accordingly, was not found in other organs such as liver, heart, intestine, kidney, brain, etc.

In comparison to their littermates, CD40L Tg mice exhibited retarded growth, cachexia, and decreased survival rates (Fig. 2, A and B). ~80% of the heterozygous offspring of CD40L Tg mice developed spontaneous dermatitis at an average age of 47 d (Fig. 2 C). The onset of dermatitis first became apparent by the reddening and thickening of the ears followed by progressive inflammation usually encompassing the ears, snouts, and often the upper thorax in the majority of the mice (Fig. 2, D and E). Homozygous CD40L Tg mice were extremely frail and developed additional massive skin alterations on tails, neck, paws, and sometimes back (Fig. 2 F) which became evident at 3–4 wk of age. These animals did not breed, were particularly prone to cachexia, and died within 3–5 mo after birth.

Histologic Analyses of Skin. Histopathological analysis of H&E-stained sections of the ear or tail skin of CD40L Tg mice revealed various abnormalities (Fig. 3, B and C). The skin was characterized by a thickened acanthotic epidermis and hyperkeratosis. Single necrotic keratinocytes were sporadically detectable within the basal cell layers. The dermal connective tissue was fibrotic with increased numbers of fibroblasts. There was a massive mixed infiltrate of lymphohistiocytic cells within the dermis although far fewer neutrophils than would be expected from a bacterial infection were present. Focally, the number of hair follicles and sebaceous glands was reduced and some keratinous cysts were present in association with a surrounding foreign body reaction. Tissue from the paws was examined for possible inflammation of the joints. However, no signs of arthritis were found (data not shown).

To further characterize the cells infiltrating the skin, immunohistochemical staining of cryostat sections of ears exhibiting mild inflammation was performed. The dermis of Tg mice contained large numbers of $CD4^+$ and $CD8^+$ T cells (Fig. 3, E, F, H, and I) that were not detectable in the skin of nonTg mice (Fig. 3, D and G). In addition, large numbers of $BM8^+$ cells were also present in the skin of Tg mice, whereas only a few $BM8^+$ cells were evident in the dermis of nonTg mice (Fig. 3, J–L). This antibody reacts with mature tissue macrophages as well as with LCs in the skin. Interestingly, in comparison to the control mice, there were increased numbers of large $CD11c^+$ DCs in the dermis of CD40L Tg mice but rarely in the epidermis (Fig. 3, N and O).

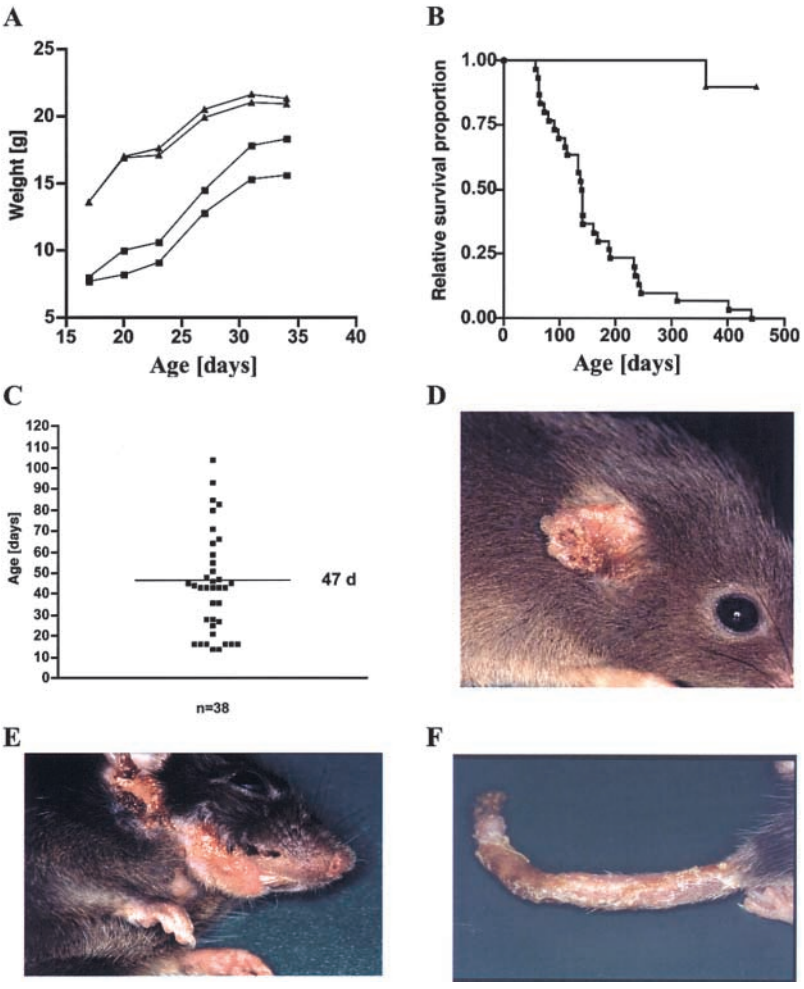

Figure 2. (A) Growth of male CD40L Tg mice and their nonTg littermates, as assessed by their weight gain. Tg mice are represented by squares and their littermates by triangles. (B) Lifespan of CD40L Tg and nonTg mice plotted using Kaplan and Meier curves. Tg mice ($n = 30$) are depicted by squares and their littermates ($n = 10$) by triangle. (C) Plot of the age (d) at which skin lesions began to develop ($n = 38$). The mean age of 47 d is indicated by the horizontal line. (D) Typical skin lesions of the ears and (E) snout of a heterozygous CD40L Tg mouse. (F) Typical skin disorder of the tail of a homozygous mouse.

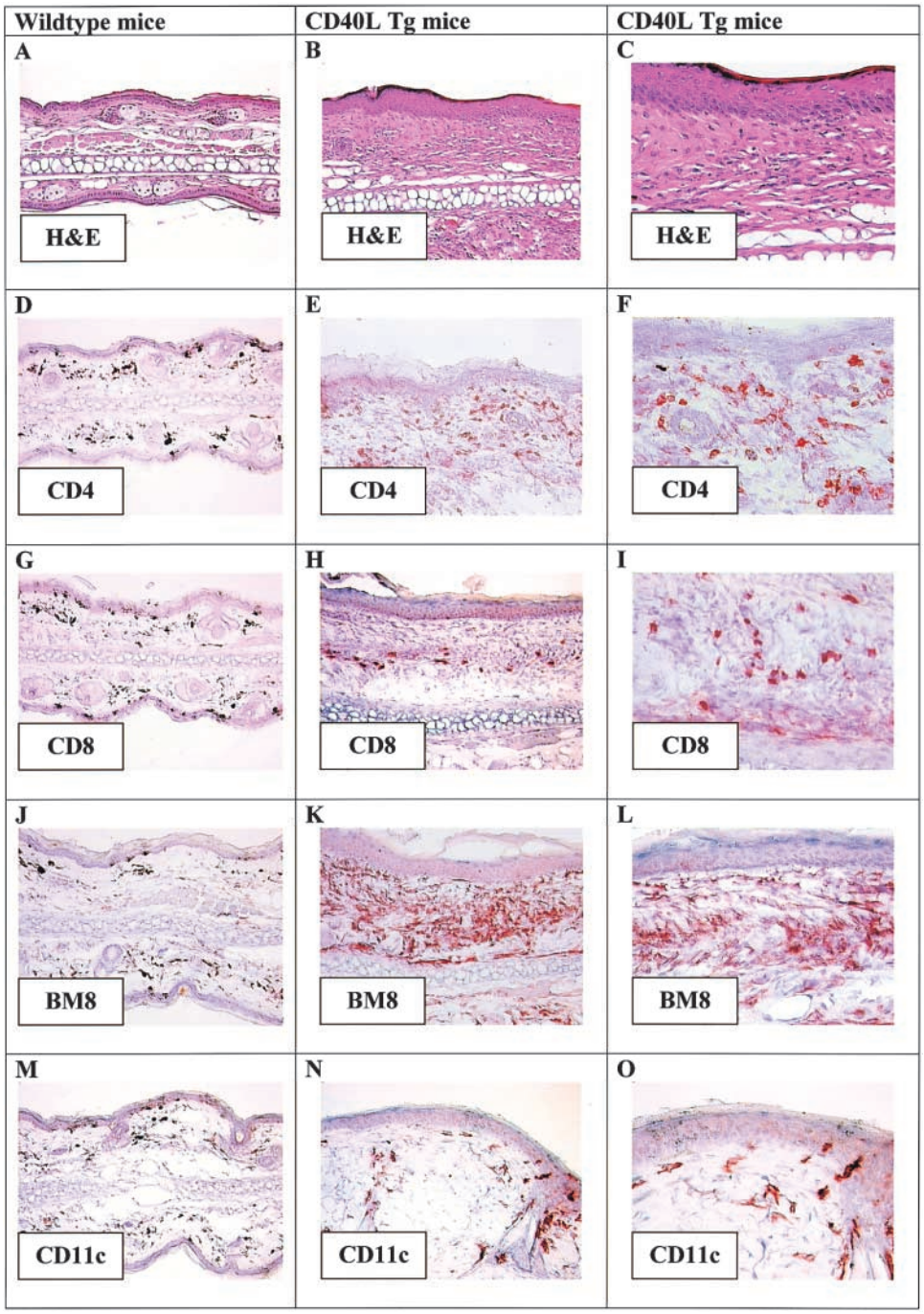

Figure 3. H&E-stained paraffin-embedded sections of (A) ears from wild-type mice (original magnification: 20×) and (B and C) ears from CD40L Tg mice. Original magnification: 200×; 400×. Immunohistochemical staining of cryostat sections using antibodies directed against (D–F) CD4, (G–I) CD8, (J–L) BM8, and (M–O) CD11c. Original magnification: 20×; 200×; 400×.

As CD40L is one of the most potent activators of DCs, epidermal ear sheets of mice were stained for I-A to visualize LCs in situ. Interestingly, in comparison to wild-type mice which have a uniform network of LCs in the epidermis (Fig. 4 A), CD40L Tgs had a consistent reduction in LCs of >90% (Fig. 4 B, wild-type: 642 ± 125 LC/mm^2; CD40L Tg: 27 ± 22 LC/mm^2). Furthermore, in large areas a "cobblestone" pattern of I-A-positive–activated keratinocytes was seen as has been described for other Tg mice harboring immunomodulatory genes in the skin (CD80, reference 14; CD54, reference 15; IFN-γ, reference 9). The majority of visual fields was totally devoid of LCs. In rare isolated areas, occasional very large I-A$^+$ LCs were observable (Fig. 4, C and D). Electron microscopic analysis corroborated the results obtained by immunofluorescence and immunohistochemical analyses of the epidermal sheets of the skin sections as the epidermis did not contain any cells identifiable as LCs (data not shown). Young CD40L Tg mice (day 18) also showed the same marked reduction of epidermal LCs compared with age-matched controls (18-d-old wild-type: 683 ± 42 LC/mm^2; 18-d-old CD40L Tg mice: 23 ± 9 LC/mm^2).

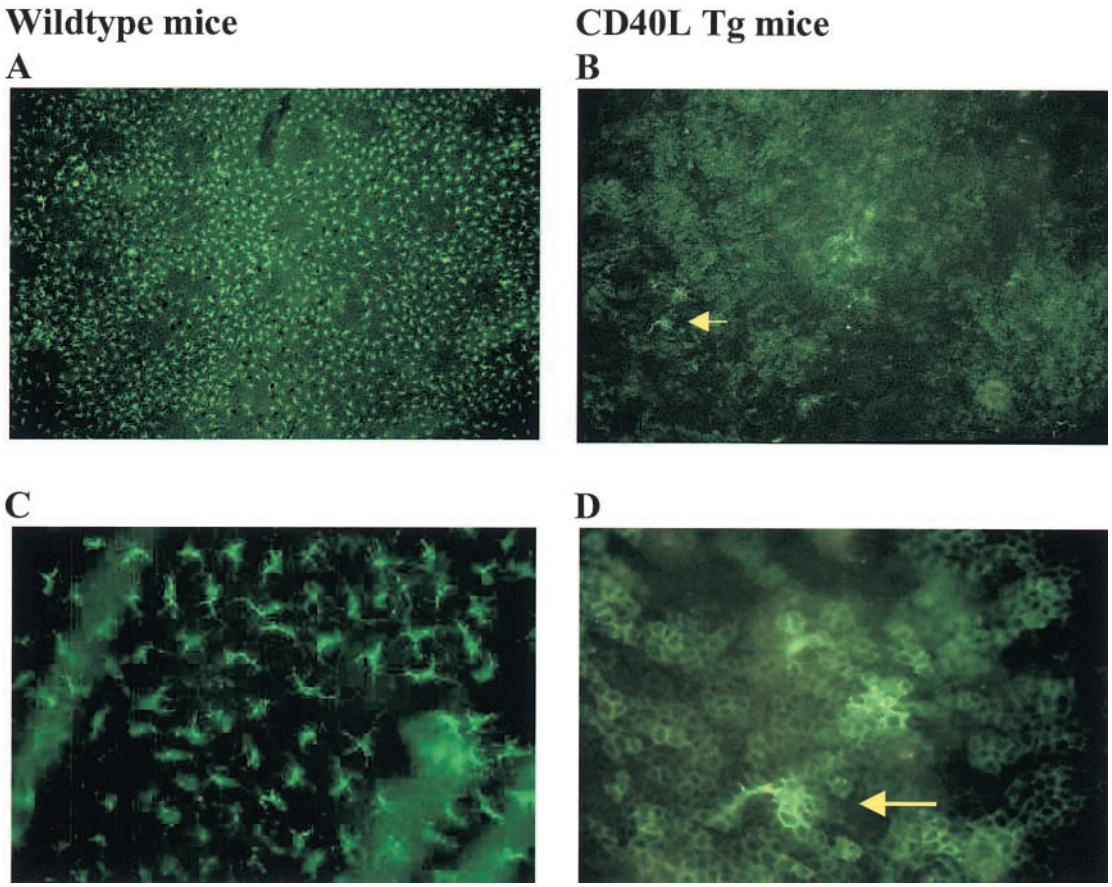

Figure 4. Fluorescence microscopy of I-A-positive cells in the earskin of nonTg (A and C; original magnification 100× and 400×, respectively), and CD40L Tg mice (B and D; original magnification 100× and 400×, respectively). The yellow arrow points to LCs that are depicted at higher magnification (400×) in D. Note the "cobblestone" pattern of the I-A-positive keratinocytes.

Again, the majority of visual fields were totally devoid of LCs in day 18 Tg epidermis before onset of disease was discernible (data not shown).

LCs are the major epidermal cell type that transports antigen to the LNs and primes naive T cells. The absence of DCs in the epidermis and the increase of activated DCs in the dermis of Tg mice gave rise to the hypothesis that DC turnover in the skin of CD40L Tg mice is enhanced. To determine whether emigration of LCs from the skin of Tg mice was increased, the hapten FITC was painted onto the ears of 5–6-wk-old mice that had not yet fully developed the skin lesions of the ears or their littermates and the LNs were analyzed 18 h later. As shown in Fig. 5, flow cytometric analyses of CD11c and FITC double-positive cells revealed higher numbers of double-positive cells in the LNs of Tg mice as compared with nonTg mice, suggesting that more hapten-laden LCs had reached the LNs in the CD40L Tg mice.

CD40L Tg Mice Develop LN Hyperplasia and Splenomegaly. CD40L Tg mice typically exhibited hyperplasia of the regional LNs that drained inflamed areas. These invariably included the cervical LNs. The sizes of other LNs were comparable to those of wild-type mice. Furthermore, 58% of the Tg mice exhibited splenomegaly.

The cellularity of the cervical LNs of CD40L Tgs was greatly increased, and there was an overall increase in the cell numbers within each individual leukocyte population as examined by flow cytometry (Table I). Upon evaluation of the relative percentages of the various leukocyte populations within the LNs, we found a decrease in the $CD4^+$, $CD8^+$, and $CD62L^+$ populations when comparing CD40L Tg mice to wild-type animals. The relative percentages of the expression of other cell surface markers were consistently increased and particularly evident in the $CD19^+$ (B cell), $CD11c^+$ (DC), and $I\text{-}A^+$ populations.

To ascertain whether Tg expression had an effect on LN architecture, paraffin sections were stained with H&E. In addition, cryostat sections were stained for DCs (CD11c), the B cells (CD19), and for T cells (CD4 and CD8). The LNs of the CD40L Tg mice were very large and there were many large germinal centers, consistent with the increase in B cell numbers (Fig. 6 A; not all data shown). Both the germinal centers of the spleen and the LNs were characterized by follicular hyperplasia with increased mantle zone thickness. Some $CD4^+$ T cells were not only dispersed throughout the T cell areas of the LNs but could also be found within the B cell rich follicles of CD40L Tg mice. In addition, large numbers of $CD11c^+$ DCs were ev-

Table I. *Weight, Cellularity, and Flow Cytometric Analyses of Cervical LNs and Spleens*[a]

	LN		Spleen	
Marker	Wild-type	CD40L Tg	Wild-type	CD40L Tg
Weight (mg)	9.4 ± 1.0	76.3 ± 8.2	107.6 ± 8.3	238.1 ± 40.5
Number of cells	$3.0 \times 10^6 \pm 0.9$	$43.8 \times 10^6 \pm 8.7$	$79.3 \times 10^6 \pm 11.6$	$307.1 \times 10^6 \pm 53.6$
BM8[b]	4.3 ± 1.1	9.9 ± 1.4	6.6 ± 0.7	10.5 ± 1.3
CD4	30.7 ± 2.8	16.5 ± 1.1	17.8 ± 1.1	15.7 ± 1.4
CD8	17.5 ± 1.8	10.2 ± 0.8	10.5 ± 1.2	9.6 ± 1.4
CD11c	3.8 ± 0.4	8.5 ± 1.3	8.9 ± 0.8	11.9 ± 0.9
CD19	29.9 ± 4.6	41.8 ± 2.6	57.9 ± 2.3	37.2 ± 3.6
CD40	24.3 ± 3.4	40.3 ± 2.4	63.9 ± 1.9	51.4 ± 3.7
CD62L	69.4 ± 2.8	54.7 ± 4.8	49.6 ± 5.5	43.4 ± 4.4
CD86	8.2 ± 3.5	13.3 ± 2.5	8.2 ± 1.2	14.3 ± 2.9
I-A	35.3 ± 8.4	48.0 ± 3.9	62.6 ± 8.2	39.6 ± 4.6

[a]Data represent mean weights and cellularity of $n \geq 12$ animals.
[b]Six mean percentages of positive cells ± SEM of $n \geq 6$ mice.

ident (Fig. 6 A). As CD40L activates DCs, flow cytometric analyses of the DC population revealed an increase in the activation markers I-A, CD80, and CD86 (Fig. 6 B) as well as strongly increased numbers of $CD11c^+/I\text{-}A^+$, $CD11c^+/CD80^+$, and $CD11c^+/CD86^+$ cells (Table II). Cervical LN hyperplasia was also seen in young 18-d-old CD40L Tg mice before the overt onset of disease with increased $CD19^+$ (B cell), $CD11c^+$ (DCs), and $I\text{-}A^+$ populations (data not shown).

Differences in the makeup of the spleen of Tg mice compared with wild-type mice were not as pronounced, except for the B cell population. In contrast to the LN, there was a dramatic decrease in the relative percentages of $CD19^+$ and $I\text{-}A^+$ cells in CD40L Tg mice when compared with littermate control mice. On the other hand, the relative percentages of $CD4^+$ and $CD8^+$ T cells were similar in both strains. Similar to the LN composition, there was an increase in the relative percentages of $CD11c^+$ and $BM8^+$ populations in the CD40L Tg mice. Analysis of production of the cytokines TNF-α, IL-4, IL-6, IL-12, and IFN-γ in LN, spleen, epidermis, and serum did not reveal any significant differences between Tg and nonTg mice (data not shown).

Although other LNs from the CD40L Tg mice, such as the intraperitoneal LNs, were not enlarged, LN hyperplasia could have been attributable to higher levels of soluble CD40L in the serum of Tg mice. Therefore, Western blot analysis of serum proteins was conducted. There were no

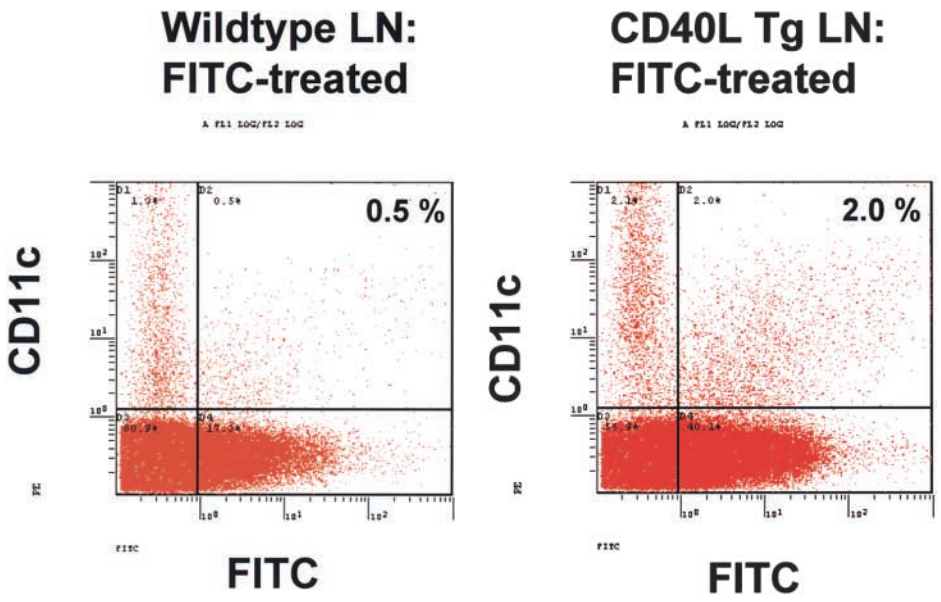

Figure 5. Flow cytometric analyses of retroauricular LNs 18 h after FITC treatment. FITC-treated LN cells from CD40L Tg mice or their nonTg littermates were stained for CD11c.

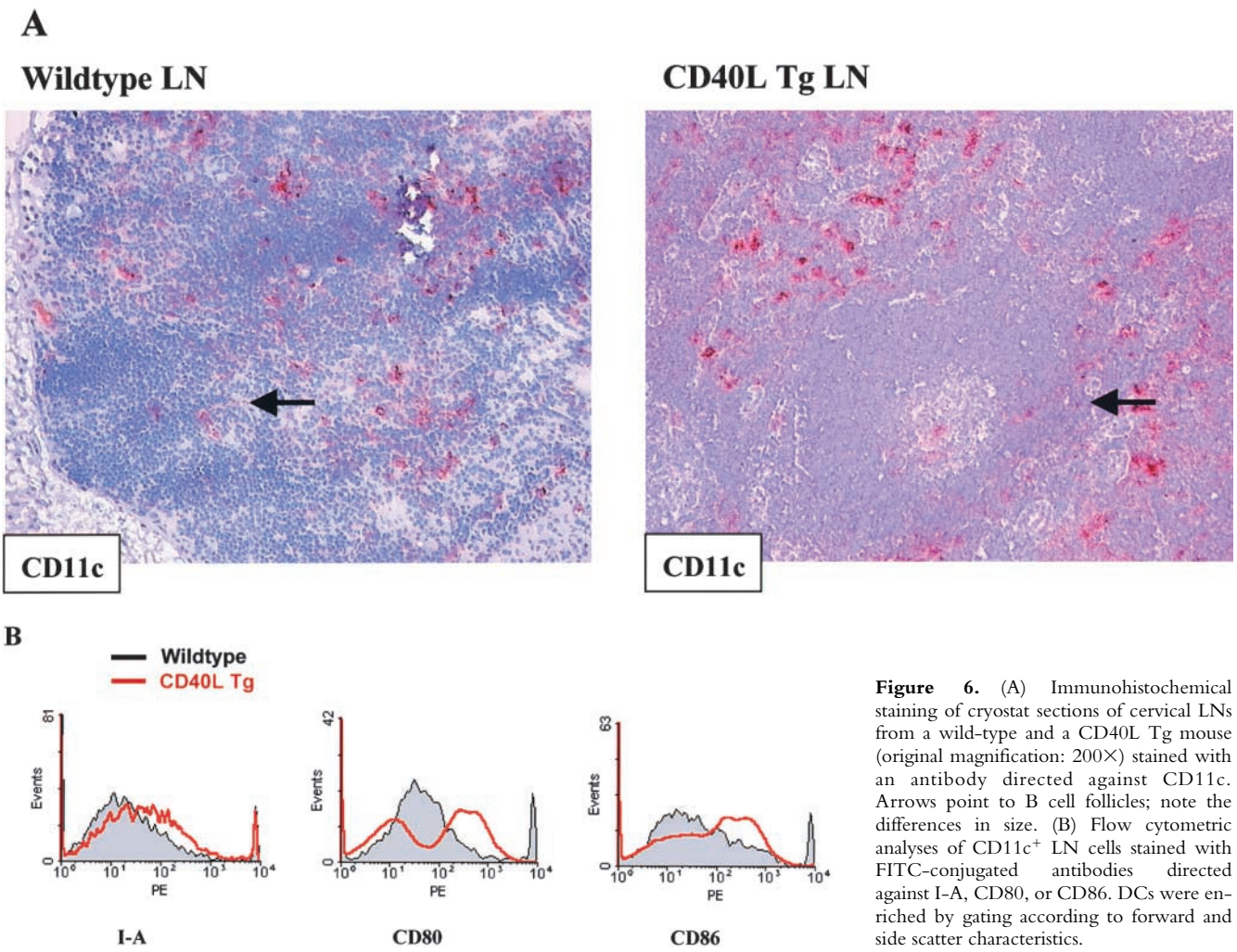

Figure 6. (A) Immunohistochemical staining of cryostat sections of cervical LNs from a wild-type and a CD40L Tg mouse (original magnification: 200×) stained with an antibody directed against CD11c. Arrows point to B cell follicles; note the differences in size. (B) Flow cytometric analyses of $CD11c^+$ LN cells stained with FITC-conjugated antibodies directed against I-A, CD80, or CD86. DCs were enriched by gating according to forward and side scatter characteristics.

detectable differences in soluble CD40L levels between the serum of Tg mice and the serum of control mice (data not shown). Furthermore, the addition of 50 μl of serum of a CD40L Tg mouse with a strong phenotype to 3×10^6 bone marrow–derived DCs per 3 milliliter cultivated with GM-CSF and IL-4 at day 6 did not generate any major differences in the expression of the cell surface markers I-A, CD86, CD40, ICAM-1, or CD11c in comparison to serum from nonTg animals as determined by flow cytometric analyses 2 d later (data not shown). These data suggest that systemic concentrations of bioactive CD40L were below the threshold required for in situ activation of DCs.

Table II. *Analysis of the DC Population of the LNs*

	Number of cells per LN	
	Wild-type	CD40L Tg
$CD11c^+/I\text{-}A^+$	$\sim 0.76 \times 10^{6a}$	$\sim 7.7 \times 10^6$
$CD11c^+/CD80^+$	$\sim 0.48 \times 10^6$	$\sim 6.7 \times 10^6$
$CD11c^+/CD86^+$	$\sim 0.49 \times 10^6$	$\sim 7.9 \times 10^6$

Mean cellularity of $CD11c^+/I\text{-}A^+$, $CD11c^+/CD80^+$, and $CD11c^+/CD86^+$ cells in pooled cell suspensions of 18 wild-type (total cell number: 13.7×10^6) or 18 CD40L Tg (total cell number: 137.0×10^6) LNs.
[a]Data represent mean cellularity of ≤18 pooled LNs.

The increase in the B cell population warranted us to look for changes in the serum Igs. Compared with nonTg animals, the serum level of IgM was significantly decreased, whereas the serum levels of IgG2a, IgG2b, IgE, and particularly IgG1 were significantly increased (Fig. 7). There was no significant difference in the IgG3 and IgA serum levels between the Tg and nonTg mice.

CD40L Tg Mice Develop Systemic Autoimmunity. To determine whether the skin abnormalities of the CD40L Tg mice could possibly be the result of an autoimmune response, sera from wild-type and Tg mice were screened for ANAs using HEp-2 cells. The sera from 13 of the 15 CD40L Tg mice tested scored positive and all controls ($n = 5$) scored negative. ANAs were detectable in Tg mice as early as 5 wk of age. Although the patterns of ANA staining of CD40L Tg mice were heterogeneous, CD40L Tgs primarily exhibited antinucleolar staining with a pronounced nuclear ring. Fig. 8 shows a typical negative (Fig.

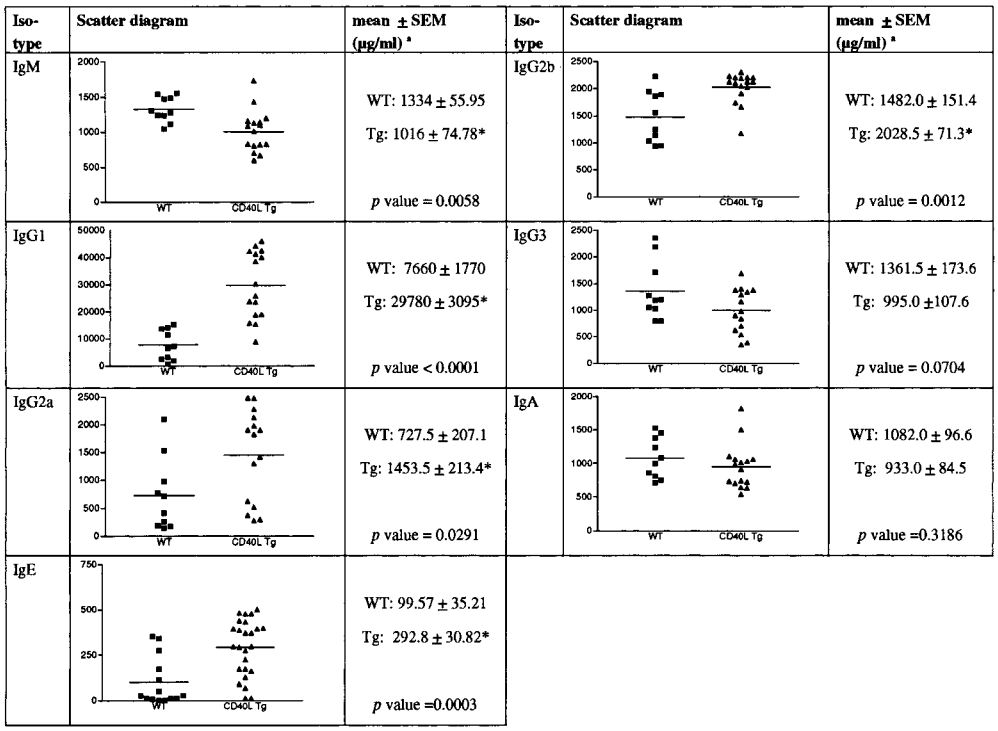

Figure 7. Ig levels in the serum of Tg and nonTg mice. Scatter diagrams and mean values ± SEM of the serum Igs tested ($n \geq 10$ mice are shown). P values are indicated. *Depicts Student's t test values, $P < 0.05$.

8 A) and positive (Fig. 8 B) staining of wild-type and CD40L Tg mice, respectively.

The nuclear rim staining pattern was indicative of the presence of anti-dsDNA antibodies. Serum samples were therefore subjected to *C. lucilidae* assays. The kinetoplast of this organism harbors large amounts of dsDNA only and reactivity of autoantibodies can be used as a specific test for the presence of anti-dsDNA autoantibodies. Of the 15 Tg animals tested, 11 exhibited staining of the kinetoplast. All control animals tested negative. Fig. 8, C and D show representative negative and positive staining of the kinetoplast resulting from indirect immunofluorescent staining of nonTg or Tg serum Igs, respectively.

Autoimmune diseases are often associated with the involvement of internal organs, in particular the kidneys and sometimes the lungs, during disease progression (20). Therefore, cryostat sections of kidneys were analyzed for the presence of renal depositions of Igs and glomerulonephritis. Immunofluorescent staining of kidneys revealed dense deposits of Igs within the mesangium of the glomeruli and within tubuli of CD40L Tg mice although only mild infiltration by inflammatory cells was evident as assessed by H&E staining. Of the 5 Tg mice tested, all exhibited Ig deposits, whereas control mice showed no significant deposits (Fig. 8, E and F). Clinically, these animals also developed proteinuria indicating impairment of renal function. In addition, the lungs of some animals exhibited pathological changes such as emphysema, fibrosis and, interstitial inflammation (Fig. 8, G and H)

Autoreactive T Cells Initiate the Skin Manifestations in Tg Mice. One of the hallmarks of autoimmunity is the presence of autoantibodies and/or autoreactive T cells that elicit tissue damage. To ascertain whether autoantibodies directed against skin components were present in the serum of Tg mice indirect immunofluorescence staining was performed. To this end, cryosections of ear or footpad skin of nonTg mice were incubated with serum from Tg and nonTg mice. Serum from Tg mice resulted in a distinct intracellular staining of the basement membrane and basal keratinocytes of the epidermis which was not observed when serum from control mice was used (Fig. 8, I and J). Thereupon, serum transfer was performed in order to determine whether the autoantibodies themselves play a fundamental role in the initiation of the skin lesion development. Neither serum from Tg nor serum from nonTg mice elicited the development of skin disorders in nonTg mice (data not shown).

These results pointed to a role of autoreactive T cells in the generation of the CD40L Tg phenotype. To determine whether this was indeed the case, T cells were prepared from spleens as well as cervical and submandibular LNs of Tg mice draining inflamed skin or control mice. From these T cells $CD4^+$ or $CD8^+$ cells were purified as described and injected into the tail vein of sex-matched recipient mice. Other recipients received a mixture of both $CD4^+$ and $CD8^+$ T cells. All recipient mice developed skin lesions similar to those of CD40L Tg mice at an average of 18 plus or minus 4 d after injection of mixed $CD4^+$ and $CD8^+$ T cells originating from the CD40L Tg mice (data not shown). We next tested whether transferable pathology is induced by highly purified $CD4^+$ or by $CD8^+$ T cells. Interestingly, only recipients of $CD8^+$ T cells from Tgs (Fig. 9, C and D), but not recipients of $CD4^+$ T cells from Tgs (Fig. 9, A and B) developed skin lesions at an average

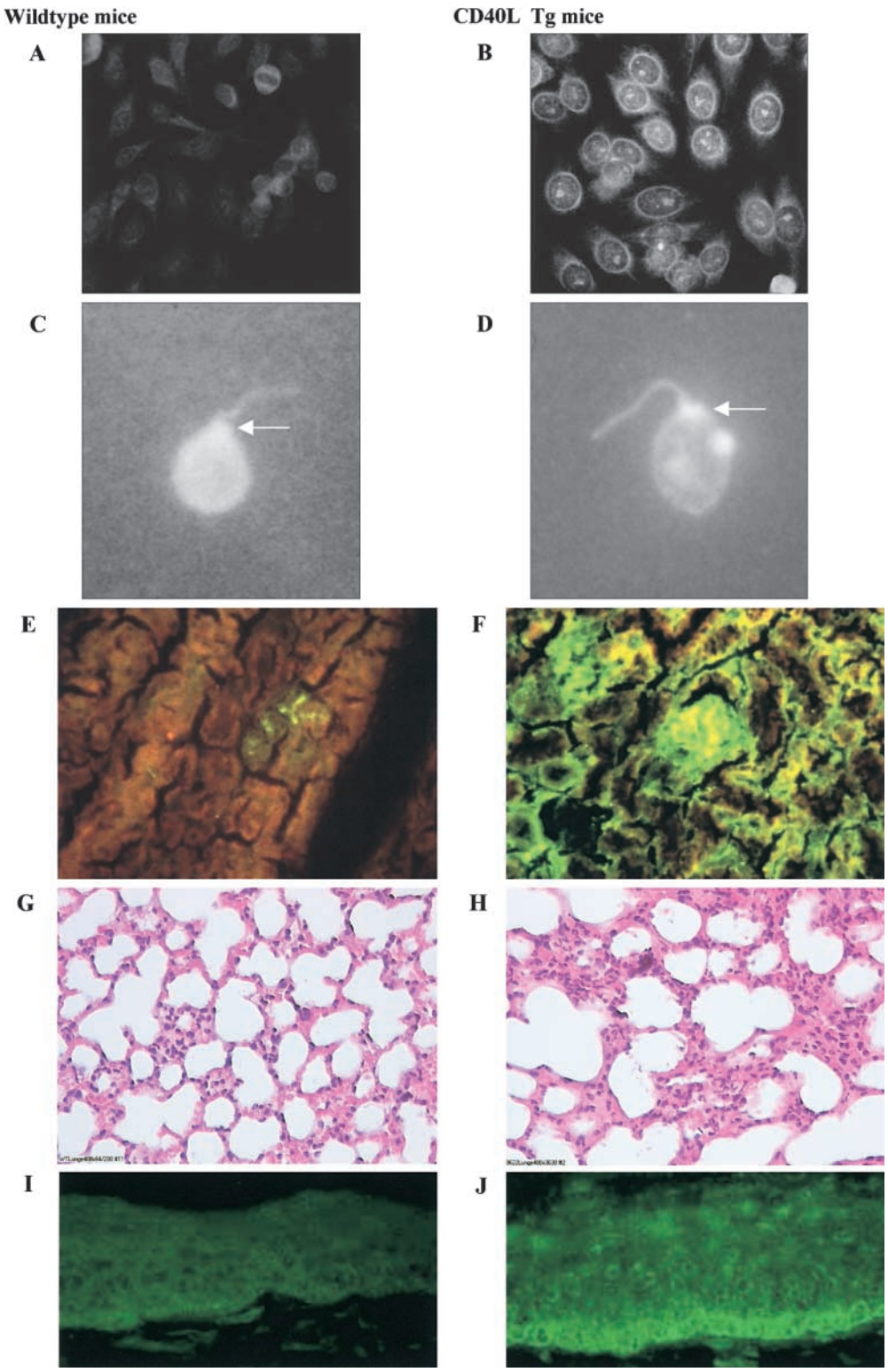

Figure 8. (A) Typical negative indirect fluorescent staining of HEp2 cells incubated with serum from control mice. (B) Typical positive staining of HEp2 cells incubated with serum from a CD40L Tg mouse. Original magnification 400×; serum dilution 1:80. (C) Typical negative indirect fluorescent staining of *C. lucilidae* cells incubated with serum from control mice. (D) Typical positive staining of the kinetoplast (arrow) of *C. lucilidae* cells incubated with serum from a CD40L Tg mouse. Original magnification: 1,000×; serum dilution 1:40. (E and F) Immunofluorescence staining of renal deposits of Igs. (G and H) H&E staining of lung tissue. (I and J) Indirect immunofluorescent staining of immune deposits in nonTg mouse footpad skin after incubation with serum from a nonTg mouse (I) or a CD40L Tg mouse (J).

of 7 plus or minus 2 d, suggesting that upon transfer, the $CD8^+$ T cells are primarily able to induce autoimmune skin inflammation. The recipient mice did not develop skin disorders when the T cells isolated from nonTg mice were used for injection. These data indicate that among the $CD8^+$ T cells, autoreactive T cells are indeed present, which are directed against components of the skin and that this specific autoreactivity is transferable.

To elucidate the role of the B cells in the elicitation of the autoimmune response, CD40L Tg mice were backcrossed into the B cell–deficient mouse strain J_HT (21). B cell–deficient CD40L Tg mice exhibited a similar inflam-

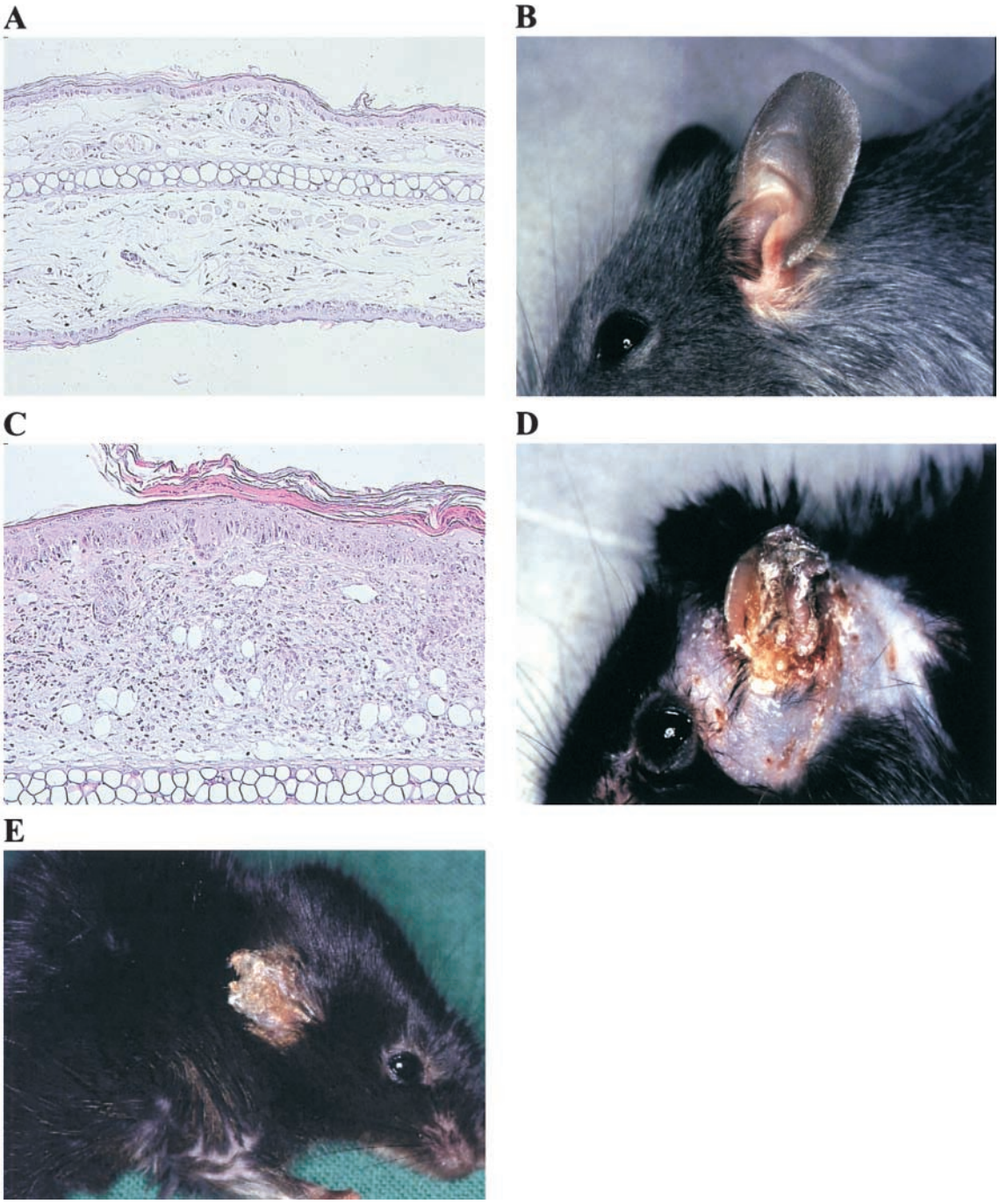

Figure 9. (A and B) Ear of a nonTg mouse 4 wk after transfer of $CD4^+$ T cells from CD40L Tg mice. H&E-stained histology section. Original magnification 200×. (C and D) Typical skin pathology of a nonTg mouse 4 wk after transfer of $CD8^+$ T cells from CD40L Tg mice. H&E-stained histology section. Original magnification: 40×. (E) Ear of a B cell–deficient (J_HT) CD40L Tg mouse.

matory phenotype with the typical involvement of the ears, snouts, paws, and tail (Fig. 9 E).

Discussion

The current study was initiated to investigate the effects of continuous activation of tissue resident DCs. Thus, Tg mice were generated that overexpress CD40L in the basal keratinocytes of the epidermis. These mice acquired a striking phenotype with severe spontaneous inflammatory skin lesions, a 90% reduction in LC numbers in the ear-skin, hyperplasia of the lymph nodes draining from inflamed areas, and a high mortality rate. Surprisingly, these animals also developed systemic autoimmunity as made evident by the presence of autoantibodies and autoreactive T cells.

The degree of the reduction in LC numbers within the skin was surprising. This might be due to impaired immigration of LCs into the epidermis, enhanced activation-induced apoptosis of LCs in situ, or increased migration of CD40L-activated LCs from the skin to the LN. To this end, McLellan et al. recently reported that mature DCs are induced to undergo apoptosis after cross-linking by MHC class II (22). Although keratinocytes of CD40L Tg mice expressed MHC class II, the same group demonstrated that pretreatment of DCs with an agonistic anti-CD40 antibody rendered DCs completely resistant to MHC class II–induced apoptosis. This data argues against enhanced apoptosis of the LCs in the skin. A role in the migration of LCs to the LNs has recently been ascribed to CD40L (23). LCs of $CD40L^{-/-}$ mice failed to migrate out of the skin after contact sensitization and this defect was correctable by injection of an agonistic anti-CD40L antibody. In agreement with this, the converse effect was evident in our CD40L Tg mice, which further substantiates the role of CD40L in the migration of DCs. Moreover, the increase in the $CD11c^{+}$ population within the dermis, the increased numbers of $CD11c^{+}$ cells within the LN, the increased numbers of FITC-positive DCs in the LNs after FITC sensitization as well as increased migratory capacities of CD40L-treated DCs (24) all might suggest that LC migration is enhanced in the CD40L Tg mice.

The predominant proportion of CD40L Tg mice developed spontaneous dermatitis between 4-6 wk after birth. The skin was characterized by hyperkeratosis, sporadic single cell necrosis of keratinocytes, a dense dermal infiltrate of lymphohistiocytic cells, and dermal fibrosis. Dermatitis occurred although the animals were housed under specific pathogen free–conditions excluding the involvement of exogenous pathogens in the onset of disease. These histological features are congruent with a local autoimmune response against the skin and can be also be found in human autoimmune skin disorders such as cutaneous lupus erythematosus (25, 26).

Autoimmune disorders are characterized by the failure of the immune system to discriminate between self-determinants and foreign antigens. According to Drexhage et al., two major criteria define autoimmune disease. (i) IgG autoantibodies and/or autoreactive T cells specific for antigens of the particular organ or organ system must be present, which in turn trigger the development of morphological lesions. (ii) A similar manifestation of disease can be induced by the transfer of autoantibodies or the autoreactive T cells (27). Our findings indicate that T cells are the primary effector cells involved in the development of local autoimmunity in our model system as only the transfer of T cells from CD40L Tg mice and not the transient presence of transferred autoantibodies resulted in the development of local autoimmune dermatitis in the recipient mice. In other models of autoimmunity, tissue damage only occurred when some sort of local inflammatory stimulus was present (28). Not even IFN-γ–overexpressing mice, which develop flaky skin lesions, hypopigmented hair, ANAs, and nephritis were reported to have autoreactive T cells (10). In the skin, weak stimuli such as low-dose UV-irradiation, scratching, and even stretching of the skin has been reported to induce the release of proinflammatory cytokines, which might explain why adoptive transfer of autoreactive T cells from Tg mice causes spontaneous pathology in wild-type recipients (29). Importantly, B cells did not seem to be involved in this process as B cell–deficient/CD40L Tg mice also develop chronic dermatitis.

Surprisingly, overexpression of CD40L in the epidermis not only led to the local autoimmune skin inflammation, but also to the development of a systemic autoimmune disease as evidenced by the presence of ANAs, anti-dsDNA antibodies, and the typical involvement of internal organs. Whether autoreactive T cells upon transfer into recipient mice on their own are capable of inducing systemic autoimmunity will be interesting to see and investigations are currently being performed to address this aspect. To this end, long-term observation periods of recipients of CD40L Tg T cells are being performed to see whether systemic autoimmunity will develop. It was proposed that the activation status of APCs is a cardinal factor defining the outcome of immunity versus autoimmunity (30). In particular in a recent report, stimulation of APCs via ligation of CD40 plays a role in "breaking" tolerance (31). Our study strongly supports this concept. We speculate that CD40L-stimulated LCs possibly internalize autoantigens, present them to T cells, and thus may initiate autoantigen-induced T cell proliferation which in turn could lead to the autoreactive skin inflammation. Whether the LCs activated in the skin by the Tg expression of CD40L were able to directly induce CTL activity against self-antigens thereby eliciting the autoimmune manifestations remains to be seen. No detectable production of inflammatory cytokines was found by keratinocytes from CD40L Tg mice, probably because in contrast to human keratinocytes, which constitutively express CD40, murine keratinocytes do not (32).

A number of pathological immune disorders are associated with aberrant CD40–CD40L signaling and document the key role of this receptor–ligand pair in immune responses. The human hyper IgM syndrome, an X-linked immunodeficiency, in which a genetic alteration has rendered the CD40L molecule nonfunctional, is characterized by deficiencies in the induction of somatic mutations resulting in high serum levels of IgM and little or no IgG, IgA, or IgE antibodies (33). The opposite effect was seen in the CD40L Tg mice. These mice had a significant reduction in their IgM serum levels and significantly increased levels of IgG1, IgG2a, IgG2b, and IgE. Moreover, these mice had a considerable increase in B cells numbers and hyperplasia of the LNs draining from affected skin. These effects did not result from detectable increased serum levels of sCD40L in the serum Tg mice. Furthermore, LN hyperplasia was limited to LNs draining inflamed areas substantiating the evidence that no considerably increased amounts of sCD40L were in the serum. This suggests that other factors resulting from CD40L overexpression in the skin could be responsible for the isotype switching and the B cell proliferation. DCs themselves can directly enhance B

cell proliferation since human DCs were shown to enhance proliferation of activated B cells by a three to sixfold in vitro (34). Furthermore, studies with CD40 knockout mice revealed that DCs can also prolong B cell survival as well as enhance their proliferation (35). In a recent study, DCs genetically modified to produce CD40L were able to induce B cell–dependent humoral immunity in CD4 T cell–deficient mice (36). Hence, the increase in the B cell population of the Tg mice is also indicative of a direct influence of the increased numbers of DCs within the LN.

In this study, several lines of evidence suggest that the continuous activation of epidermal LCs by CD40L may lead to the development of chronic skin inflammation and the subsequent development of systemic autoimmunity. The data furthermore indicate a possible role for tissue-resident DCs in the induction of autoimmunity. CD40L Tg mice exhibit aspects of mixed connective tissue disease. This disease is an overlap syndrome that includes aspects of lupus erythematosus, scleroderma, and/or dermatomyositis (20, 24, 37). Analogously, CD40L Tg mice exhibit the speckled type pattern of antinuclear antibodies, anti-dsDNA antibodies, visible linear depositions at the dermoepidermal junction after indirect immunofluorescent staining, in addition to renal, lung, and skin manifestations that are also found in mixed connective tissue disease. In this context, it is important to mention that CD40–CD40L signaling has also been implicated in several human autoimmune disorders (3, 38). Studies have revealed that activated T cells from patients with systemic lupus erythematosus or scleroderma have a prolonged expression of CD40L when compared with healthy control groups (39, 40). Furthermore, in systemic lupus erythematosus patients disease activity is directly associated with elevated plasma levels of CD40L (41). Mori et al. also reported the findings that in the lesional epidermis, the expression of HLA-DR antigens by epidermal DCs was reduced and fewer $CD1a^+$ DCs (LCs) were present in comparison to normal skin (42), which is consistent with the extremely reduced numbers of LCs in the epidermis of CD40L Tg mice. The pathological findings in CD40L Tg mice therefore suggest that these Tgs represent a potentially interesting animal model for studying mixed connective tissue disease. Moreover, they have the potential of being an excellent model for dissecting the T cell and Ig/B cell–dependent pathways leading to autoimmune disease development.

We thank Dr. Elaine Fuchs, Howard Hughes Medical Institute, Chicago, IL, for providing the K14 expression cassette, Immunex for supplying the CD40L cDNA, Dr. Udo Wehmeier, University of Wuppertal, Wuppertal, Germany, for his help in sequencing the plasmids, Dr. Michael Raghunath, University of Münster, for his help in some of the photographic work as well as Dr. Hermann Herbst, University of Münster, for his comments on the LNs and spleens. We also thank Dr. Werner Muller, Gesellschaft für Biotechnologische Forschung, Braunschweig, Germany, for providing the J_HT mice and Birgit Pers as well as Maik Voskort for excellent technical assistance. We are also grateful to Dr. Matthias Gunzer, University of Münster, for providing the T cell purification protocol.

This project was funded by grants GR1022/7-1 and SFB 293B1 (to S. Grabb) from the German Research Association (Deutsche Forschungsgemeinschaft) and grant IMF119839 (to S. Beissert) from the University of Münster, School of Medicine.

Submitted: 17 January 2001
Revised: 22 June 2001
Accepted: 17 July 2001

References

1. Banchereau, J., and R.M. Steinman. 1998. Dendritic cells and the control of immunity. *Nature*. 392:245–252.
2. Schoenberger, S.P., R.E. Toes, E.I. van der Voort, R. Offringa, and C.J. Melief. 1998. T-cell help for cytotoxic T lymphocytes is mediated by CD40-CD40L interactions. *Nature*. 393:480–483.
3. van Kooten, C., and J. Banchereau. 2000. CD40-CD40 ligand. *J. Leukoc. Biol*. 67:2–17.
4. Grewal, I., and R. Flavell. 1998. CD40 and CD154 in cell-mediated immunity. *Annu. Rev. Immunol*. 16:111–135.
5. Armitage, R.J., W.C. Fanslow, L. Strockbine, T.A. Sato, K.N. Clifford, B.M. Macduff, D.M. Anderson, S.D. Gimpel, T. Davis-Smith, C.R. Maliszewski, et al. 1992. Molecular and biochemical characterization of a murine ligand for CD40. *Nature*. 357:80–82.
6. Vassar, R., M. Rosenberg, S. Ross, A. Tyner, and E. Fuchs. 1989. Tissue-specific and differentiation-specific expression of a human K14 keratin gene in transgenic mice. *Proc. Natl. Acad. Sci. USA*. 86:1563–1567
7. Saitou, M., S. Sugai, T. Tanaka, K. Shimouchi, E. Fuchs, S. Narumiya, and A. Kakizuka. 1995. Inhibition of skin development by targeted expression of a dominant-negative retinoic acid receptor. *Nature*. 374:159–162.
8. Grabbe, S., K. Steinbrink, M. Steinert, T.A. Luger, and T. Schwarz. 1995. Removal of the majority of epidermal Langerhans cells by topical or systemic steroid application enhances the effector phase of murine contact hypersensitivity. *J. Immunol*. 155:4207–4217.
9. Carroll, J.M., T. Crompton, J.P. Seery, and F.M. Watt. 1997. Transgenic mice expressing IFN γ in the epidermis have eczema, hair hypopigmentation and hair loss. *J. Invest. Dermatol*. 108:412–422.
10. Seery, J.P., J.M. Carroll, V. Cattell, and F.M. Watt. 1997. Antinuclear autoantibodies and lupus nephritis in transgenic mice expressing interferon γ in the epidermis. *J. Exp. Med*. 186:1451–1459.
11. Pior, J., T. Vogl, C. Sorg, and E. Macher. 1999. Free hapten molecules are dispersed by way of the bloodstream during contact sensitization to fluorescein isothiocyanate. *J. Invest. Dermatol*. 113:888–893.
12. Wang, B., L. Zhuang, H. Fujisawa, G.A. Shinder, C. Feliciani, G.M. Shivji, H. Suzuki, P. Amerio, P. Toto, and D.N. Sauder. 1999. Enhanced epidermal Langerhans cell migration in IL-10 knockout mice. *J. Immunol*. 162:277–283.
13. Tang, H.L., and J.G. Cyster. 1999. Chemokine up-regulation and activated T cell attraction by maturing dendritic cells. *Science*. 284:819–822.
14. Williams, I.R., R.J. Ort, and T.S. Kupper. 1994. Keratinocyte expression of B7-1 in transgenic mice amplifies the primary immune response to cutaneous antigens. *Proc. Natl. Acad. Sci. USA*. 91:12780–12784.
15. Williams, I.R., and T.S. Kupper. 1994. Epidermal expression of intercellular adhesion molecule 1 is not a primary inducer

of cutaneous inflammation in transgenic mice. *Proc. Natl. Acad. Sci. USA*. 91:9710–9714.
16. Wang, X., S. Zinkel, K. Polonsky, and E. Fuchs. 1997. Transgenic studies with a keratin promoter-driven growth hormone transgene: prospects for gene therapy. *Proc. Natl. Acad. Sci. USA*. 94:219–226.
17. Rauschmayr, T., R.W. Groves, and T.S. Kupper.1997. Keratinocyte expression of the type 2 interleukin 1 receptor mediates local and specific inhibition of interleukin 1-mediated inflammation. *Proc. Natl. Acad. Sci. USA*. 94:5814–5819.
18. Guo, L., Q.C. Yu, and E. Fuchs. 1993. Targeting expression of keratinocyte growth factor to keratinocytes elicits striking changes in epithelial differentiation in transgenic mice. *EMBO J.* 12:973–986.
19. Ford, G.S., B. Barnhart, S. Shone, and L.R. Covey. 1999. Regulation of CD154 (CD40 ligand) mRNA stability during T cell activation. *J. Immunol.* 162:4037–4044.
20. Roell, N.R., and M.J.D. Goodfield. 1998. The connective tissue diseases. *In* Rook/Wilkinson/Ebling Textbook of Dermatology. R.H. Champion, J.L. Burton, D.A. Burns, and S.M. Breathnach, editors. 6th ed. Blackwell Science Ltd., Oxford, UK. pp. 2545–2547.
21. Gu, H., Y. Zou, and K. Rajewsky. 1995. Independent control of immunoglobulin switch recombination at individual switch regions evidenced trough Cre-loxP-mediated gene targeting. *Cell*. 73:1155–1164.
22. McLellan, A., M. Heldmann, G. Terbeck, F. Weih, C. Linden, E.B. Bröcker, M. Leverkus, and E. Kämpgen. 2000. MHC class II and CD40 play opposing roles in dendritic cell survival. *Eur. J. Immunol.* 30:2612–2619.
23. Moodycliffe, A.M., V. Shreedhar, S.E. Ullrich, J. Walterscheid, C. Bucana, M.L. Kripke, and L. Flores-Romo. 2000. CD40-CD40 ligand interactions in vivo regulate migration of antigen-bearing dendritic cells from the skin to draining lymph nodes. *J. Exp. Med.* 191:2011–2020.
24. Labeur, M.S., B. Roters, B. Pers, A. Mehling, T.A. Luger, T. Schwarz, and S. Grabbe. 1999. Generation of tumor immunity by bone marrow-derived dendritic cells correlates with dendritic cell maturation stage. *J. Immunol.* 162:168–175.
25. Sontheimer, R. 1999. Lupus erythematosus. *In* Fitzpatrick's Dermatology in General Medicine. I.M. Freedberg, A.Z. Eisen, K. Wolff, K.F. Austen, L.A. Goldsmith, S.I. Katz, and T.B. Fitzpatrick, editors. 5th ed. Vol. II. McGraw Hill, New York. pp. 1993–2009.
26. Weedon, D. 1998. Skin Pathology. Harcourt Publishers Limited, Hong Kong.
27. Drexhage, H.A., F.G.A. Delemarre, K. Rodosevic, and P.J.M. Leenen. 1998. Dendritic cells in autoimmunity. *In* Dendritic Cells: Biology and Clinical Applications. M. Lotze, and A. Thompson, editors. Academic Press, San Diego, CA. pp. 361–511.
28. Ludewig, B., B. Odermatt, A.F. Ochsenbein, R.M. Zinkernagel, and H. Hengartner. 1999. Role of dendritic cells in the induction and maintenance of autoimmune diseases. *Immunol. Rev.* 169:45–54.
29. Kupper, T.S. 1990. Immune and inflammatory processes in cutaneous tissues. Mechanisms and speculations. *J. Clin. Invest.* 86:1783–1789.
30. Matzinger, P. 1994. Tolerance, danger, and the extended family. *Annu. Rev. Immunol.* 12:991–1045.
31. Garza, K.M., S.M. Chan, R. Suri, L.T. Nguyen, B. Odermatt, S.P. Schoenberger, and P.S. Ohashi. 2000. Role of antigen-presenting cells in mediating tolerance and autoimmunity. *J. Exp. Med.* 191:2021–2027.
32. Coutant, K.D., P. Ulrich, H. Thomas, A. Cordier, and A. Brugerolle de Fraissinette. 1999. Early changes in murine epidermal cell phenotype by contact sensitizers. *Toxicol. Sci.* 48:74–81.
33. Notarangelo, L.D., M. Duse, and A.G. Ugazio. 1992. Immunodeficiency with hyper-IgM (HIM). *Immunodefic. Rev.* 3: 101–121.
34. DuBois, B., B. Vanbervliet, J. Fayette, C. Massacrier, C. van Kooten, F. Briere, J. Banchereau, and C. Caux. 1997. Dendritic cells enhance growth and differentiation of CD40-activated B lymphocytes. *J. Exp. Med.* 185:941–951.
35. Wykes, M., and G. MacPherson. 2000. Dendritic cell-B-cell interaction: dendritic cells provide B cells with CD40-independent proliferation signals and CD40-dependent survival signals. *Immunology*. 100:1–3.
36. Kikuchi, T., S. Worgall, R. Singh, M.A. Moore, and R.G. Crystal. 2000. Dendritic cells genetically modified to express CD40 ligand and pulsed with antigen can initiate antigen-specific humoral immunity independent of $CD4^+$ T cells. *Nat. Med.* 6:1154–1159.
37. Maddison, P.J. 2000. Mixed connective tissue disease: overlap syndromes. *Baillièr's Clin. Rheumatol.* 14:111–124.
38. Banchereau, J., F. Bazan, D. Blanchard, F. Briere, J.P. Galizzi, C. van Kooten, Y.J. Liu, F. Rousset, and S. Saeland. 1994. The CD40 antigen and its ligand. *Ann. Rev. Immunol.* 12:881–922.
39. Koshy, M., D. Berger, and M.K. Crow. 1996. Increased expression of CD40 ligand on systemic lupus erythematosus lymphocytes. *J. Clin. Invest.* 98:826–837.
40. Valentini, G., M.F. Romano, C. Naclerio, R. Bisogni, A. Lamberti, M.C. Turco, and S. Venuta. 2000. Increased expression of CD40 ligand in activated $CD4^+$ T lymphocytes of systemic sclerosis patients. *J. Autoimmun.* 15:61–66.
41. Kato, K., E. Santana-Sahagun, L.Z. Rassenti, M.H. Weisman, N. Tamura, S. Kobayashi, H. Hashimoto, and T.J. Kipps. 1999. The soluble CD40 ligand sCD154 in systemic lupus erythematosus. *J. Clin. Invest.* 104:947–955.
42. Mori, M., N. Pimpinelli, P. Romagnoli, E. Bernacchi, P. Fabbri, and B. Giannotti. 1994. Dendritic cells in cutaneous lupus erythematosus: a clue to the pathogenesis of lesions. *Histopathology*. 24:311–321.